The impact of network topology on the performance of multi-channel single-radio mesh networks

Tânia Calçada, Manuel Ricardo
INESC Porto, Faculdade de Engenharia, Universidade do Porto
Porto, Portugal
{tcalcada,mricardo}@inescporto.pt

Abstract

This paper addresses a 802.11 mesh network used to extend Internet access, where mesh nodes simultaneously serve as access points to unmodified clients. The use of multiple channels improves the performance of these networks but significant challenges arise when nodes are limited to a single-radio interface to form the mesh network. In particular, the assignment of mesh nodes to channels results on the creation of multiple sub-networks, one per channel.

This paper identifies the relevant topological characteristics of sub-networks resultant from the channel assignment and studies, through simulation, the impact and relative importance of those characteristics on the maximal throughput enabled by the mesh network.

Abstract

– Mesh networks, multi-channel, channel assignment, single-radio, node density, hidden nodes, miss ratio.

I. Introduction

Wireless mesh networks are emerging as a low-cost solution for broadband Internet access. A mesh node is a wireless packet switch that may accumulate the function of access point. These nodes are interconnected by wireless links and, together, they enable redundant paths and help increasing the network reliability. More about wireless mesh networks can be found in [2].

This paper addresses the network scenario represented in Figure 1, used to extend the access to the Internet, and it is similar to the scenario addressed by IEEE 802.11s [6]. In this scenario, mesh nodes are expected to have two wireless cards with independent of-the-shelf radio interfaces running the standard MAC 802.11 protocol; one radio interface operates as an access point and the other is used to interconnect the node to the mesh network. Special mesh nodes are wireline connected to the infra-structured network acting as gateways to the Internet.

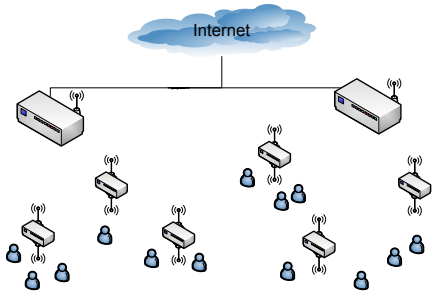

Fig. 1. Mesh network scenario deployed to extend Internet access, where nodes form a mesh network and simultaneously serve as access points to unmodified clients. Special mesh nodes are wireline connected to the infra-structured network, acting as gateways to the Internet.

The fundamental access method of the IEEE 802.11 MAC is a Distributed Coordination Function (DCF) known as Carrier Sense Multiple Access with Collision Avoidance (CSMA/CA). For a node to transmit, it first senses the medium to determine if another node is transmitting. If the medium is not busy, the transmission proceeds; otherwise, the node defers until the end of the current transmission,where it tries to transmit the frame after a random waiting time. A refinement of the method may be used to further minimize collisions; transmitting and receiving nodes exchange short control frames, Request To Send (RTS) and Clear To Send (CTS), to determine if the medium is idle prior to data transmission.

As the number of active nodes in a wireless network increases, the number of frames transmitted by each node falls down since these nodes are sharing a wireless medium of finite capacity [5]. This problem is more critical on highly loaded scenarios, where long deferring times are introduced. Network capacity increases with the number of channels in use as shown in [12], [10].

In [4], the authors show that severe inter radio interference problems arise when more than two wireless network interface cards 802.11 are active in a single node, even if they work in orthogonal channels; the authors also show that non self interfering multi radio 802.11 nodes can have up to two radios.

There is significant work done in channel assignment strategies for single-radio and multi-radio mesh networks [3]. Multi-radio approaches promise high throughputs since multiple transmissions can occur simultaneously on each node using different channels. Few works, however, exist about channel assignment strategies for single-radio mesh networks. A survey is available in [3], where most of the approaches presented stand on dynamic channel switching which require dedicated MAC layer protocols and tight time synchronization between nodes. Other proposals, [13] and [14], address single radio scenarios and they assign all nodes on a path to a common channel, not demanding changes on MAC layer. On these protocols, the assignment of different channels to nodes leads to multiple sub-networks, one for each configured channel. In [13] is presented a joint channel assignment and routing protocol where each node uses the same channel for long periods of time; the protocol aims to increase the network performance by reducing the load in each sub-network which is achieved by reducing the active path length. However, it is not proved that by just reducing path length more efficient networks are obtained. The approach used in [14] increases throughput by reducing number of contending flows on a channel, which is achieved by reducing the node density; first it determines the sets of nodes belonging to intersecting flows, and then different channels are assigned to sets of contending nodes. However, reducing contention as in [14] makes the network less connected and more susceptible to the occurrence of collisions caused by hidden nodes; this strategy is not satisfactory in Internet access scenarios because collisions occur more frequently when nodes in the neighborhood of intersecting nodes (e.g. gateways) are hidden from each other, despite facing less contention.

Our work considers nodes with two radio interfaces, one of them used by the access point to provide access to stations, what leads us to a single-radio mesh network. We assign all nodes on a path to a common channel, creating multiple sub-networks when multiple channels are used; this strategy is also used in [13] and [14]. The wireless network performance depends on the sub-networks performance which, in turn, depends on topology characteristics such as neighbor node density, hop count, and hidden nodes. The identification of metrics related to topological characteristics, the evaluation of their impact on network performance, and the analysis of their relative importance when designing a channel assignment algorithm is the problem addressed in this paper. For that purpose, we defined a set of experiments with arbitrary channel assignments in a 6x6 lattice topology network. We used ns-2 simulations and, based on the results obtained, we have identified the relevant topology characteristics that have impact on the throughput of the mesh network.

This work provides two main contributions:

1) Identification of simple network topology metrics that are related to the performance of mesh networks and can be used for deciding about channel assignment in wireless mesh networks. The metrics identified are the following: a) mean hop count; b) neighbor node density, which is the mean number of neighbors of a mesh node; c) $miss\,ratio$, which synthesizes the number of hidden nodes on the network; d) number of nodes in the 1st Ring, which are the nodes directly connected to gateway; e) mean number of hidden nodes on the 1st Ring; f) 1st Ring $miss\,ratio$.
2) Evaluation of the impact of these metrics have on the performance of the network, namely: a) the number of nodes directly connected to the gateway and the mean number of hidden nodes on links to the gateway, which are by far the most important metrics; b) the $miss\,ratio$ metric, which also has an high impact; c) the mean hop count and neighbor node density, which have low impact on the network performance.

The rest of the paper is organized as follows. Section II characterizes network topology characteristics and derives a set of topology related metrics. Section III defines the problem to be solved and describes the methodology used in our study. Section IV presents the results of this study. Section V concludes the paper, presents future work and identifies possible applications of our results.

II. Topology Characteristics

A. Hop Count

An upper bound for the throughput of a node in a mesh network is given in [9]. The analysis is not limited to a specific MAC, but the result can be applied to IEEE 802.11. The concept of bottleneck collision domain is introduced there by defining it as the geographical area of the network that enables an upper bound on the amount of data that can be transmitted in the network. This concept enables the derivation of the impact the mean number of hops H has in a given network, when all nodes are sources of flows with the same packet rate of $\lambda\,packet/s$ destined to a common sink.

Let us consider the topologies of Figure 2 which combine a chain of N_c nodes and a star of $N - N_c$ nodes; when $N_c = 0$ the network has

star topology; when $N_c = N - 1$ the network is a chain topology. In this case, the mean hop Count H is given by Eq.1,

$$H = \frac{\sum_{n=1}^{N_c} n + [(N - N_c) \cdot (N_c + 1)]}{N} = \frac{(N_c + 1)\,(N - N_c/2)}{N} \quad (1)$$

where the first addend refers to the N_c nodes on the chain part of the network, and the second addend refers to the the $N - N_c$ nodes on the star part of the network.

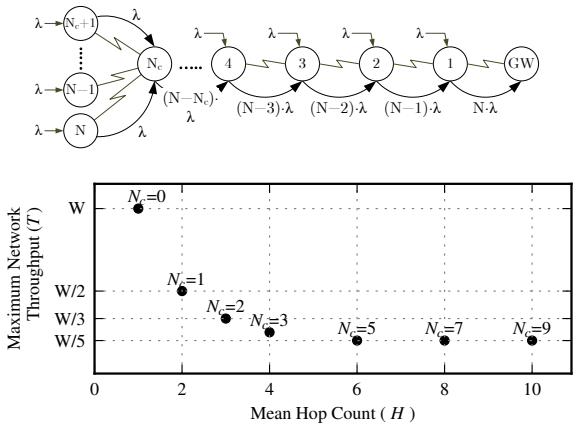

Fig. 2. Topologies combining a chain of N_c nodes and a star of $N - N_c$ nodes. The throughput of star-chain topology networks is represented as a function of the mean hop count H from each node to the gateway assuming N=∞.

When $N_c \leq 4$, all links are on the same collision domain [9]; the traffic on this collision domain is the traffic on links on the star part of the network given by $\lambda(N - N_c)$ and the traffic on the chain part of the network given by $\lambda \sum_{n=0}^{N_c-1} (N - n)$. The collision domain cannot transport more traffic than the channel data rate W as presented by Eq. 2

$$W \geq \lambda(N - N_c) + \lambda \sum_{n=0}^{N_c-1} (N - n) \geq \lambda N \frac{(N_c + 1)\,(N - N_c/2)}{N}),\ N_c \leq 4 \quad (2)$$

By using H from Eq. 1 in Eq. 2 it is possible to obtain $W \geq \lambda N H$ for $N_c \leq 4$. Therefore, the maximum throughput available for each node is $\lambda_{max} = W/(NH)$ and the upper bound of network throughput $T = N\lambda_{max}$ is given by Eq. 3.

$$T \leq \frac{W}{H},\ N_c \leq 4 \quad (3)$$

When $N_c > 4$, the bottleneck collision domain on star-chain networks of Figure 2 is the collision domain of link 2-3 composed by links {GW-1, 1-2, 2-3, 3-4, 4-5} [9]. Each collision domain has to forward the sum of the traffic of its links. In this case, the collision domain of link 2-3 has to forward $\lambda \cdot [(N-4)+(N-3)+(N-2)+(N-1)+N] = \lambda \cdot (5N-10)$. The collision domain cannot forward more traffic than the channel data rate W, what means that $W \geq \lambda \cdot (5N - 10)$. Therefore, the maximum throughput available for each node is $\lambda_{max} = W/(5N-10)$ and the upper bound of network throughput $T = N \cdot \lambda_{max}$ is given by Eq. 4.

$$T \leq \frac{WN}{5N - 10},\ N_c > 4 \quad (4)$$

The maximum achievable throughput given by Eq. 3 and Eq. 4 is represented in the lower part of Figure 2 as a function of H for $N = \infty$; this graph shows that, for these topologies, the maximum achievable throughput T tends to the inverse of H. However, T does not always vary with H; for $H \geq 5$, which correspond to $N_c \geq 4$, T is fixed to $W/5$. Therefore, the inference of the maximum achievable throughput is not possible for a generic network by just knowing H.

B. Neighbor Node Density

Neighbor node density is defined as the mean number of nodes in the receiving range of a node. Assuming a CSMA/CA MAC, the higher the number of active nodes is in a region the less will be the throughput per node due to contention. Consider the network topology on Figure 3(a) containing $N = 6$ nodes. The lines represent links between nodes; if a line is not represented between two nodes, these nodes cannot sense each other's transmissions. Each node generates a data flow destined to Node F which is the gateway of this network. Data is transmitted through the paths defined by the links represented by lines with arrows. The neighbor node density d is calculated as the mean number of neighbors a node has. In this case we have nodes A, B, E and F with 2 neighbors, and nodes C and D with 3 neighbors, thus the neighbor node density for Figure 3(a) is $d = [(4 \times 2) + (2 \times 3)]/6\, nodes = 2.33$.

The interference models presented in [5] capture the interference between a pair of links in a wireless network. Interference is caused by

active nodes on the vicinity of both the sender and receiver of a link. The physical and protocol models of [5] are referred in relevant studies of multichannel in mesh networks such as [12], [10], [11], [7]. In these models the throughput λ obtainable by a node is shown to decrease with the increase of the neighbor node density as given by

$$\lambda = \Theta\left(\frac{W}{\sqrt{n \log n}}\right) [5] \quad (5)$$

where W is the channel capacity and n is the number of nodes in the network, supposing that the n nodes are located in a region of area 1 m^2.

In [11], Kuo et al. prove that the throughput λ of each node grows asymptotically as fast as a function $f(d)$ of neighbor node density d, $\lambda = \Theta(f(d))$, where $f(d)$ is given by Eq. 6 and c is a constant. Authors argument that $f(d)$ has two factors that characterize a trade-off between hop progress on the numerator and contention on the denominator. The numerator $1 - (d^{-1}e^{-d/c})$ shows that the throughput increases with the neighbor node density; when there are more neighbors around a node, the probability that the next node on the multi-hop path is closer to the destination increases, and so does the hop progress. A large neighbor node density d thus leads to a smaller path hop count for each flow, which in turn reduces the amount of traffic to be relayed by each node in the network, allowing each node to spend more time transmitting its own traffic. On the other hand, the denominator shows that a large neighbor node density also introduces more contentions in the access to the wireless channel by the nodes in the receiving range. When d is small, the numerator has more significance than the degradation due to contention, however when d grows the contention starts dominating the maximum throughput.

$$f(d) = \frac{1 - (d^{-1}e^{-d/c})}{d} [11] \quad (6)$$

The study in [11] does not consider collisions caused by hidden nodes or simultaneous transmissions which are highly related with neighbor node density. The works reported in [7] and [1] address these problems. Packet collisions due to simultaneous transmissions are expected to increase with the increase of neighbor node density since it is more likely that two or more nodes of a neighborhood transmit at the same time slot. However, collisions due to hidden nodes can decrease when the neighbor node density increases since the number of hidden nodes can also decrease, what implies that for some topologies the throughput can increase when neighbor node density is high, as shown for the networks we study and represent in Figure 5(a).

C. Hidden Nodes

The hidden node problem is partially solved by the RTS/CTS mechanism of IEEE 802.11 on wireless local area networks. However in multi-hop networks it is proved [15] that hidden mesh nodes cause severe problems on network performance even when the RTS/CTS mechanism is used, since it does not solve the mesh hidden node problem and it increases the network overhead, leading to performance degradation.

For a given topology, the mean number of hidden nodes can be measured by averaging the number of hidden nodes of each active link in the network. The number of hidden nodes of a link is the number of neighbors of the link's receiver that are not neighbors of the link's transmitter. For instance, on Figure 3(a) there are 5 active links which are the links used to transmit data represented by arrows. Node D is hidden from link A-B, C and F are hidden from B-D, F is hidden from C-E, E is hidden from D-F, and D is hidden from E-F. The mean number of hidden nodes of the topology of Figure 3(a) is $(1+2+1+1+1)/5 = 1.2$ nodes. Attempts to analytically characterize the impact of hidden nodes on multi-hop networks are described in [7] and [1].

In [7], the authors introduce the $miss\,ratio$ metric which is a global measure of the severity of the hidden nodes in the overall network. To describe the $miss\,ratio$ metric, the authors first define a set of graphs that capture the physical interferences and the carrier sensing constraints between links in a network: s-graph, tc-graph, and rc-graph. In these graphs a vertex represents a wireless link. The s-graph can be used to capture the physical interference constraints graphically; an s-graph edge between vertex 1 and vertex 2 indicates that, in order to prevent future collisions, link 1 (node T_1 to node R_1) must be capable of forewarning link 2 (node T_2 to node R_2) not to transmit after link 1 initiates a transmission. The tc-graph models the transmitter-side carrier sensing; an tc-graph edge between vertex 1 and vertex 2 means that link 1 can and will forewarn link 2 not to transmit when link 1 is transmitting. The rc-graph models the receiver-side carrier-sensing constraints; an rc-graph edge between vertex 1 and vertex 2 indicates that R_2 will ignore T_2 transmission when the R_2 already senses a transmission on link 1. For the network of Figure 3(a) s-graph, tc-graph and rc-graph are presented in Figures 3(b), 3(c), and 3(d)

Using the graphs described above it is possible to obtain the hidden links on the network by $\overline{TC} \cap (S \cup RC)$ where S, TC, and RC are respectively the set of edges on s-graph, tc-graph, and rc-graph. The number of hidden links is given by $N_{HN} = \left|\overline{TC} \cap (S \cup RC)\right|$. If a tc-edge does not exist

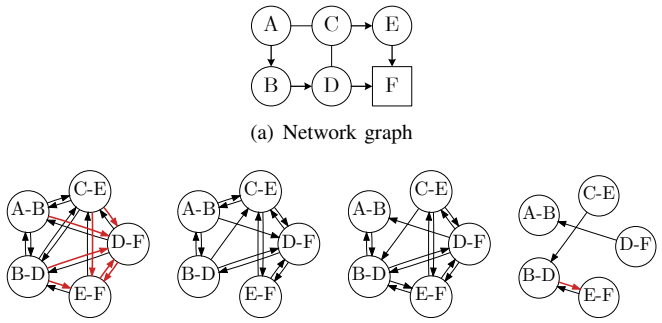

(a) Network graph

(b) s-graph (c) tc-graph (d) rc-graph (e) hidden links

Fig. 3. In the topology of (a), the square node F is the network sink; lines represent wireless connectivity and arrows represent the data path. (b) is the s-graph, (c) is the tc-graph, (d) is the rc-graph, and (e) represents the hidden nodes, for the topology shown in (a). The 1st Ring s-graph and 1st Ring hidden nodes are respectively the sub-set of s-graph and hidden links represented as red strong lines.

from link 1 to link 2, the transmission of link 1 will not be sensed by T_2. But if a rc-edge or a s-edge exists between link 1 and link 2, it indicates that either R_2 will ignore T_2 when R_2 senses a transmission on link 1 (rc-edge), or that there is physical interference from link 1 to link 2 (s-edge). In both cases, T_2 will interpret it as a collision and we can say that link 1 is hidden from link 2. The hidden links of Figure 3(a) are represented in Figure 3(e). The $miss\,ratio$ metric is then the ratio between the number of hidden links N_{HN} and the number of edges belonging to rc-graph or s-graph, as given by Eq. 7.

$$miss\,ratio = \frac{N_{HN}}{|S \cup RC|} \tag{7}$$

When $TC = \{S \cup RC\}$ there are no hidden links N_{HN} and $miss\,ratio = 0$, which is the ideal value to avoid collisions on a network. In [7], the authors do not relate $miss\,ratio$ with the network throughput. For the network on Figure 3(a), $\{S \cup RC\} = \{S\}$ and $|S| = 18$, thus $miss\,ratio = 4/18 = 0.22$.

In [1], the authors model the per-hop throughput T_h as a function of network parameters such as the communication sense range R, the number of nodes D per m^2, the expected duration of frames transmission, the propagation delay, the duration of an idle slot, the minimum MAC backoff window size, and the MAC retry limit. In [1] is shown that the number of collisions caused by hidden nodes is higher than the number of collisions caused by simultaneous transmissions; their analysis is based on graphs that plot the probability of collision caused by simultaneous transmission p_{cx}, the probability of collisions caused by hidden nodes p_{ch} and the probability of total collisions p as a function of R for a fixed number of nodes per m^2 D. [1] also provides a graph relating the per-hop throughput T_h as a function of the communication range R. Using this graph and the one relating the probabilities of collision and R, it is possible to conclude that the per-hop throughput is very influenced by the probability of collisions.

D. GW Position and Topology of GW Neighborhood

In a scenario where a mesh network is used to extend Internet broadband access, the gateway position has a great impact on the network performance. Gateway position, along with channel assignment, affects the topology characteristics described earlier in this section. Gateways on central positions of the mesh network lead to shorter paths. Gateways deployed on the edges of the mesh network, can bring benefits because the number of contending nodes around them may be reduced.

Considering the gateway as the center of the networks on the scenarios treated by our work, it is possible to define rings around the gateway. A set of nodes on the n[th] Ring indicates that the minimum path between those nodes and the gateway has n hops. Considering this concept and the 3 topology characteristics presented in the previous subsections, it is possible to derive metrics that characterize the topology on each ring.

The 1st Ring is of particular interest for this study since their nodes share and manage the bottleneck of the network which is the wireless channel around the gateway. Regarding the hop count there is no need to have a metric since all nodes on the 1st Ring are at 1 hop of the gateway. The neighbor node density around the gateway can be measured by simply checking the size of the 1st ring, which is the number of nodes at one hop distance to the gateway. The hidden nodes on the 1st Ring can either be measured by calculating the mean number of hidden nodes of 1st Ring links or by calculating the $miss\,ratio$ of the 1st Ring. The 1st Ring links are the links between the 1st Ring nodes and the gateway.

The 1st Ring $miss\,ratio$ is calculated using S_{R1}, TC_{R1} and RC_{R1} which are respectively the set of edges on s-graph, tc-graph and rc-graph which affect the gateway, as given by Eq. 8

$$miss\,ratio_{R1} = \frac{N_{HN_{R1}}}{|S_{R1} \cup RC_{R1}|} \tag{8}$$

where $N_{HN_{R1}} = \left|\overline{TC_{R1}} \cap (S_{R1} \cup RC_{R1})\right|$ is the number of links hidden from 1st Ring links. For the network on Figure 3(a), the S_{R1} and HN_{R1} are the bold red edges in Figure 3(b) and Figure 3(e), $|S_{R1} \cup RC_{R1}| = 7$ and $|HN_{R1}| = 1$ thus $miss\,ratio_{R1} = 1/7 = 0.14$.

III. Problem statement and methodology

Using multiple wireless channels in mesh networks is proven [12], [10] to improve the network performance when using an appropriate channel assignment scheme. In a single-radio mesh networks, the goal of a channel assignment algorithm is to determine in which channel should each node be working on. We recall that a single radio mesh node is a node that can use one network interface and one channel at a time for communication with the other mesh nodes. Every time a mesh node is assigned a new channel, the topology of the network changes.

We argue that the network throughput can be optimized by controlling the network topology characteristics. As seen, relevant topology metrics are the mean hop count, the neighbor node density, the mean number of hidden nodes, the $miss\,ratio$, the size of the 1st Ring, the mean number of hidden nodes on the 1st Ring, and the $miss\,ratio$ 1st Ring. These metrics change when a node is assigned to another channel. In this work, we aim to estimate the impact each metric has on the network throughput. This knowledge can be used to decide what channel shall a mesh node be assigned to.

In order to estimate the impact of the topology of a network on its performance, we carried out extensive simulation. Channel assignment scenarios were applied to a 36 node network displaced in a 6x6 lattice topology, as represented on Figure 4. The number inside a circle identifies the node. The lines represent wireless link layer connectivity.

On Figures 5 to 10, the squares represent the gateways that have a wired connection to the Internet. Dark circles in these figures represent nodes configured on a channel, and light circles represent nodes on an orthogonal channel; these two networks are interconnected through their gateways.

Each node, except the gateways, generates a traffic flow whose packets are generated by a Poisson process, that is the inter-arrival times are exponentially distributed; these packets are UDP and are destined to a node in the Internet. All packets are received by wireless links by a gateway before delivered to its final destination in the Internet. The simulation was designed to avoid packet losses between the gateway and the wired node, and a packet is considered successfully delivered upon its reception by the gateway. All the flows are configured with similar parameters, which are fixed for each simulation; each simulation was run with 10 different seeds. The parameters used in simulation are presented on the Table I. The ns-2 was used with two-ray propagation model in the physical layer, MAC DCF 802.11 in the link layer, and the Hybrid Wireless Mesh Protocol (HWMP) [6] was used to establish routes.

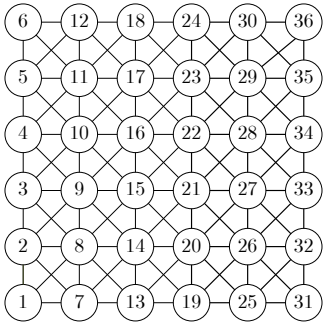

Fig. 4. 6x6 lattice used to study the impact of topology characteristics on the network throughput.

Parameter	Value
Propagation Model	two ray ground
Channel data rate	11 Mbit/s
RX Threshold	-70.2 dBm, 350 m
Node distance	176 m
Packet size	1500 bytes
RTS/CTS	ON
Max retrans retries	7
Routing	HWMP
Source type	Poisson (UDP)
WarmUp packet	256 byte
WarmUp data rate	10 packet/s
Simulation runs	10

TABLE I
Parameters used in NS-2.29 simulations.

1) Duration and warm up period: simulations run for 60 seconds, what may imply the generation of 37500 packets. During the first 3 seconds there are no data flows; this period is used to allow the HWMP routing protocol to execute the proactive tree building functionality; in this phase

a route to one of the gateways is added to each node as described in the the Proactive PREQ mechanism [6]. Between second 3 and second 4 the warm up flow takes place between each node and the gateway; this flow enables the ARP tables of each node to be filled. On second 5, the main flows start and go on until second 50. The last 10 seconds of each simulation are used to enable packets to be dequeued.

HWMP is a hop-by-hop protocol; intermediate nodes use lookup table to determine next hop based on destination. When forwarding frames through a multihop path using HWMP, intermediate nodes determine the next hop looking up for the final destination on the forwarding table. Since all flows are destined to a common sink, each node uses always the same entry of its forwarding table to forward the traffic from itself, and from the nodes that rely on it, to the gateway. Therefore, the number of active links on the network is equal to the number of nodes excluding the gateways.

2) Compared scenarios: the two channel assignment schemes A1 and A2 represented in Figure 5(a), along with a single channel scenario (A-SCh), were used as the basis scenarios to study the impact of the topology characteristics on network throughput. Scenarios B1 and B2 of Figure 6, based on A1 and A2 but with fewer nodes, were simulated to study the effect of hop count. Scenarios of Figure 7, based on A1 and A2 with larger carrier sensing range, were used to study the neighbor node density. Scenarios D1, D2, D3 and D4 of Figure 9 and scenarios A3, A4 and A5 of Figure 10 were used to study the impact of the gateway neighborhood.

IV. Results

Two channel assignment schemes were applied to the 36 node lattice network represented in Figure 4. The resulting networks are represented in Scenario A1 and Scenario A2 of Figure 5(a) where dark circles represent nodes configured on a channel, and light circles represent nodes on an orthogonal channel, forming two networks connected through their gateways. While the channel assignment scheme used in Scenario A1, minimizes the number of hops, the scheme used in Scenario A2 aims to reduce the neighbor node density.

Figure 5 also shows the throughput and topology characteristics of the two scenarios represented in Figure 5(a), and compares it with a third scenario (Scenario A-SCh) where all nodes and gateways of Figure 4 work in a common channel. Each node generates a flow towards the gateway, so 17 flows were simulated on each channel on the A1 and A2 scenarios, and 34 flows were simulated in the single channel scenario. A set of simulations were carried out. In each simulation all flows generated the same bit rate. Bit rates from $10\,kbit/s$ to $7.5\,Mbit/s$ were used. RTS/CTS handshake was also used and the CSThresh was configured to guarantee a carrier sensing range of 350 m.

Figure 5(b) presents the throughput of the network, which is defined as the sum of the bit rate received by the two gateways, divided by the number of sources of the network which is 34; for each source node debit, Figure 5(b) presents the mean of throughput and the 90% confidence interval calculated using the results of the 10 simulations runs. Topology characteristics of these scenarios are presented on Figure 5(c), and they were calculated as explained on Section II; the 90% confidence intervals of the topology metrics are also shown and indicate that the values shown are very accurate. The results on Figure 5 are compared with results from simulations with variants of scenarios A1 and A2 and discussed in the following subsections.

A. Traffic load and throughput

Low load traffic conditions are assumed when each source generates less than $120\,kbit/s$. In these conditions every channel assignment scheme, including the single channel, presents the same throughput results. In low load traffic conditions, all the packets are delivered to the destination without noticeable losses, independently of the scenario used; Figure 5(b) proves this by showing that for debits below $120\,kbit/s$, the throughput is equal to the source debits.

When the traffic load is higher than $120\,kbit/s$, the throughput starts growing slowly, in opposition to the linear growing for low loads. The networks start to loose packets and the differences of performance between the topologies start to be evident.

IEEE 802.11's theoretical data rate for each gateway is $11\,Mbit/s$, but more than 50% [8] of it is used in overhead, leaving $5.5\,Mbit/s$ per gateway available to transmit packets from 34 flows. The maximum mean data rate for each flow is $5.5\,Mbit/s \times 2\,gateways\,/\,34\,nodes = 323\,kbit/s$. Considering that each frame is forwarded through multiple hops until it reaches the gateway, the maximum achievable throughput is even lower. Therefore, it is expectable that a considerable amount of frames are lost when the sources debit is above $0.3\,Mbit/s$.

Figure 5(b) shows that Scenario A2 has a maximum throughput of $127\,kbit/s$ for the offered load of $190\,kbit/s$, what suggests the existence of an optimum offered load. For Scenario A1, the throughput increases even when it starts to loose significant amounts of data (when each node source debit is higher then $300\,kbit/s$), and it continues to grow with

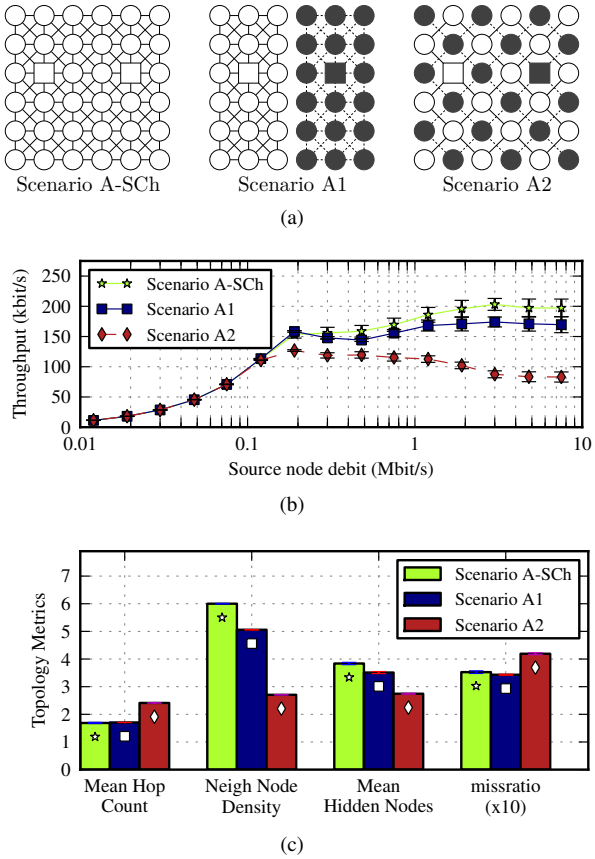

Fig. 5. (a) Network topology, (b) throughput and (c) topology metrics of two dual-channel and one single channel assignment schemes. The 90% confidence intervals of the mean throughput and topology metrics are also shown.

increasing amounts offered load until it reaches a saturation value of $170\,kbit/s$. The inefficiency of Scenario A2 for high loads is caused by hidden nodes which cause collisions. Despite the mean number of hidden nodes in Scenario A2 is lower that in the other scenarios, as shown by Figure 5(c), the neighbor node density is also lower indicating that most of the neighbors are hidden from each other, as revealed by the $miss\,ratio$ of Scenario A2, which is higher than in Scenario A1.

B. Mean hop count

An experiment was performed to understand the impact of the mean hop count on the throughput of the networks of Scenario A1 and Scenario A2. Nodes on positions 2, 4, 6, 9, 11, 27, 29, 32, 34 and 36 (refer to Figure 4) were removed from networks on both scenarios in order to get similar mean hop count; the resulting networks are Scenario B1 and Scenario B2, shown in Figure 6.

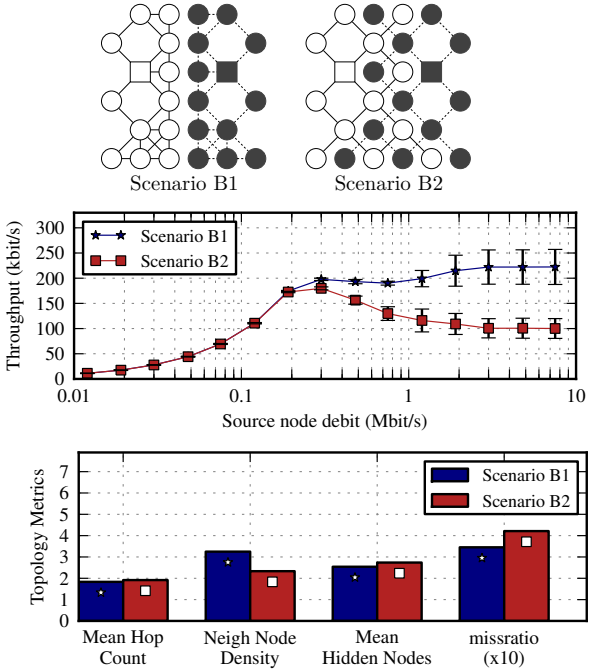

Fig. 6. The network topology, throughput with 90% confidence intervals, topology metrics of a reduced version of scenarios on Figure 5(a), where nodes on positions 2, 4, 6, 9, 11, 27, 29, 32, 34 and 36 (refer to Figure 4) were removed.

The networks of Scenarios B were subjected to the same tests and loads described before. The achieved throughputs with the correspondent 90% confidence intervals and the topology metrics are also shown in Figure 6. The shape of these graphs are similar to those presented in Figure 5 showing that the mean hop count of these networks does not have a great impact on the network performance. An increase of about 30% on the maximum throughput was observed for scenarios B1 and B2, when

compared with scenarios A1 and A2. This increase was expected since less nodes are sharing the gateways and the channel. However, the maximum total throughput of the network $T = N\lambda_{max}$ is higher on scenarios A1 and A2; $T_{A1} = 34 \times 170 = 5.78\,Mbit/s$, $T_{A2} = 34 \times 130 = 4.42\,Mbit/s$, $T_{B1} = 24 \times 220 = 5.28\,Mbit/s$, $T_{B2} = 24 \times 180 = 4.32\,Mbit/s$.

C. Neighbor node density in the single channel scenario

Figure 5(b) shows that the single channel scenario presents a throughput higher than the scenarios using two channels. This result is true when the two gateways are deployed beyond the carrier sensing range of each other. The following experiment was performed to understand the impact of increasing the carrier sensing distance on the network throughput. The networks of Figure 5(a) were configured with a carrier sensing threshold that guarantees a carrier sensing range of 550 m, which enables gateways to sense each other's transmissions. The resultant networks and their wireless connections are presented in Figure 7; these networks were subjected to the same tests and loads described before. The achieved throughputs and the topology metrics are also shown in Figure 7; the correspondent confidence intervals were omitted in order to simplify the figure, but are if the same order of length as the ones represented in Figure 5.

In the Scenario A-Sch (Single Channel) with carrier sensing range configured to 350 m (Figure 5), the two gateways are on the same channel but not on the communication range of each other, therefore they can receive traffic from neighboring nodes simultaneously. When the carrier sensing range enables the gateways to sense each other's transmissions, as in Scenario C-Sch of Figure 7, the gateways share the channel and are on the communication range of each other; it implies that gateways cannot receive packets simultaneously and there is a decrease of network throughput as shown by Figure 7, when comparing Scenario C-Sch and Scenario A-Sch.

Another remarkable result is that throughput of Scenario C1 is higher than Scenario A1 while Scenario C2 presents lower throughputs than Scenario A2, as shown by the throughput graph of Figure 7. This can be explained by the $miss\,ratio$, the mean number of hidden nodes and the neighbor node density. As shown in the topology metrics graph of Figure 7, all channel assignment schemes with wider carrier sensing range - scenarios C1, C2 and C-SCh - have neighbor node densities higher than schemes of scenarios A1, A2 and A-SCh. However, the number of hidden nodes and the $miss\,ratio$ have different behaviors for the different channel

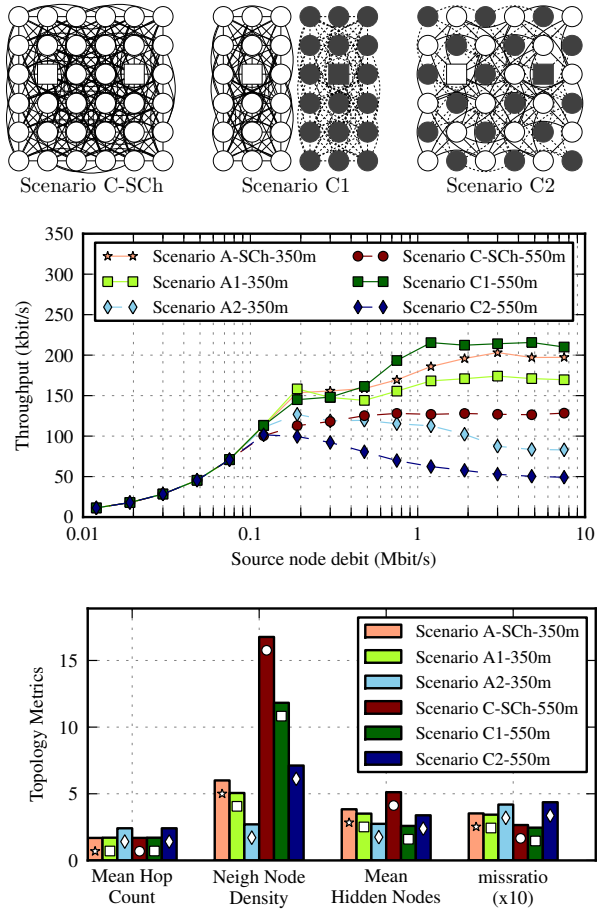

Fig. 7. Network topology when carrier sense range is 550 m using the same channel schemes of Figure 5(a). When the carrier sense range enables the gateways to sense each other's transmissions, the single channel scenario (Scenario C-Sch) performance is lower than the Scenario A-Sch. The decrease and increase respectively of hidden nodes from Scenario A1 to Scenario C1 and A2 to C2, justifies the increase and decrease on the throughput.

assignment schemes when the neighbor node density increases. When it comes to scenarios A1 and C1, the mean number of hidden nodes and $miss\,ratio$ decreases when the neighbor node density rises; for scenarios A2 and C2 as well as single channel scenarios A-SCh and C-SCh, the mean number of hidden nodes and $miss\,ratio$ increases with the neighbor

node density.

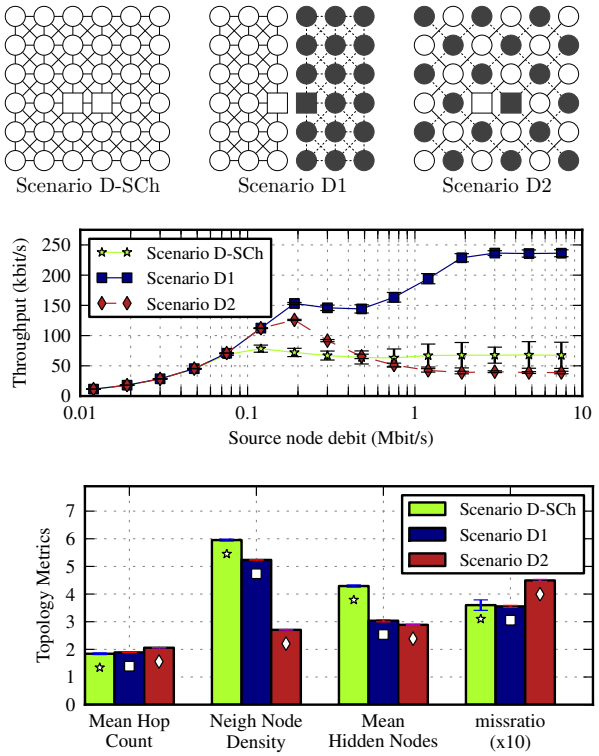

Fig. 8. Network topology, throughputs with 90% confidence intervals, and topology metrics when gateways are deployed in positions 15 and 21 on the center of the network.

D. Gateways position in the single channel scenario

In order to confirm that single channel scenarios where gateways are placed on the communication range of each other, present worst results than two channels a new experiment was made where the gateways were deployed in positions 15 and 21 (refer to Figure 4), as shown in Figure 8. The networks of Scenarios D were subjected to the same tests and loads described before. The achieved throughputs with the correspondent 90% confidence intervals and the topology metrics are also shown in Figure 8. The throughput for single channel scenario with centered gateways, Scenario D-Sch, on Figure 8 is less than half of the throughput obtained when the gateways are out of the communication range of each other (Scenario A-Sch on Figure 5(b)).

In Scenario D-Sch it is possible to have different routing paths on each simulation run. Different routing paths turns out in different $missratios$ as shown by the wider confidence interval of $missratios$ on Scenario D-Sch presented in the topology metrics graph on Figure 8. This variations on $missratio$ leads to variations on the throughput as shown by the wider confidence intervals of throughputs of Scenario D-Sch when compared with Scenario D1 and Scenario D2.

E. Size of the gateway neighborhood

In order to understand the impact of the characteristics of a gateway neighborhood, scenarios E1, E2, E3 and E4 were simulated. These scenarios, on Figure 9, show channel assignment schemes with 1, 2 and 3 nodes around the gateway. Scenarios E1 and E4 are, respectively, based on Scenarios A2 and A1 presented in Figure 5(a), moving the gateways to the corners of the lattice. Scenarios E2 and E3 are variants of Scenario E1 where the gateway neighborhood was modified to get respectively 2 and 3 nodes around the gateway.

The networks of Figure 9 were submitted the same traffic and tests described earlier. The networks throughputs with 90% confidence intervals, and the topology metrics are also presented in Figure 9.

Results in Figure 9 show that throughput depends on the 1st Ring size which is the neighbor node density around the gateway. The higher is the 1st Ring size, the higher is the throughput obtained. Also, the mean hop count and the $miss\,ratio$ shown in the topology metrics graph of Figure 9 present an inverse relationship with the observed throughputs shown in the throughputs graph; in this case the higher is the hop count and $miss\,ratio$ the lower are the throughputs obtained.

The throughput obtained in Scenario E3 and Scenario E4 are similar. Curiously, most of these two topologies metrics are different, except the size of the 1st Ring. This observation enable us to conclude that the size of the 1st Ring may have a great importance on the performance of the network.

From the 4 channel assignment schemes tested, Scenario E3 and Scenario E4 present the highest throughput. In fact, the 290 $kbit/s$ achieved is near the maximal theoretical throughput for a 34 flows destined to 2 gateways when the channel data rate is 11 $Mbit/s$, which is 323 $kbit/s$ as explained above. Additional random channel assignment schemes with 34 nodes plus 2 gateways were tested and the maximum observed

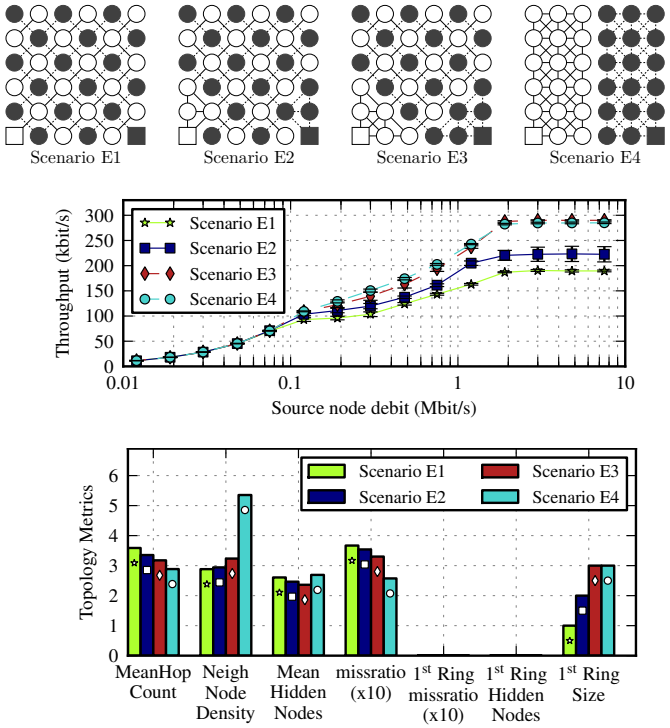

Fig. 9. Channel assignment schemes with few full connected nodes on the neighborhood of the gateway. Throughputs with 90% confidence intervals, and topology metrics are also presented.

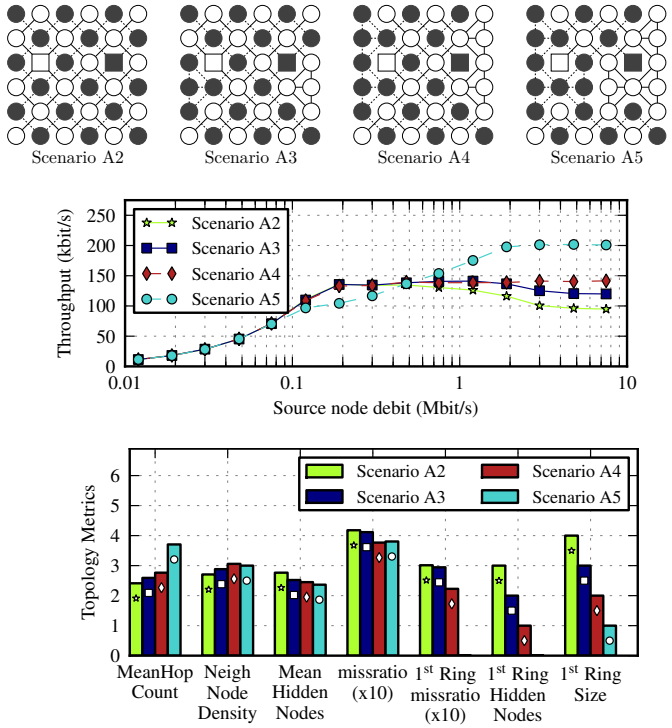

Fig. 10. Channel assignment schemes with few nodes on the neighborhood of the gateway, all hidden from each other. Throughputs with 90% confidence intervals, and topology metrics are also presented.

throughput was found always below $300\,kbit/s$ per node. All the scenarios reaching near the maximum throughput, have similar 1st Ring topology characteristics: three full connected nodes around the gateway.

F. Hidden nodes on the gateway neighborhood

In order to verify the impact of 1st Ring hidden nodes and 1st Ring $miss\,ratio$ on the network performance, the scenarios of Figure 10 were also tested. Scenarios A3, A4 and A5 are variants of Scenario A2, previously presented in Figure 5(a), where size of 1st Ring becomes respectively 3, 2 and 1. On these scenarios, all 1st Ring nodes are hidden from each other in order to verify the importance of 1st Ring size in the presence of hidden nodes around the gateway.

The networks on Figure 10 were submitted to the same traffic and tests described earlier. The networks throughputs and the topology metrics are also presented in Figure 10; the correspondent confidence intervals were omitted in order to simplify the figure, but are if the same order of length as the ones represented in Figure 9.

In opposition to what was observed in Figure 9, for Scenarios A2, A3, A4 and A5 the throughput decreases with the increase of the size of the 1st Ring, as shown in Figure 10. However, on scenarios of Figure 10, the number of hidden nodes around the gateway increases with the increase of 1st Ring size. Based on that, we conclude that the number of hidden nodes on the 1st Ring influences more the network performance than the size of the 1st Ring size.

The $miss\,ratio_{R1}$ is a $miss\,ratio$ calculated considering only the links hidden from 1st Ring links. $miss\,ratio_{R1}$ shown in the topology metrics graph of Figure 10 are clearly related with the throughput also shown in that figure. The $miss\,ratio_{R1}$ of Scenarios A2, A3 and A4 have small differences between them, while the $miss\,ratio_{R1}$ of Scenario A5 is much smaller. Notably, this relationships are also present between the throughputs of Scenarios A2, A3, A4 and A5 on Figure 10.

Scenario A5 has the best performance presented in Figure 10 because it has a single node on the 1st Ring and therefore does not have nodes hidden from this single link to the gateway. However, the throughput of Scenario A5 does not reach the maximum achievable throughput observed at Scenarios E3 and E4 on Figure 9 because a single link of Scenario A2 is not able to make hay of channel capacity as the three 1st Ring links of Scenarios E3 and E4 .

By comparing Scenarios E4, E3 of Figure 9 with Scenario A3 of Figure 10, we can understand the behavior of scenarios with similar number nodes on the 1st Ring, but different number on hidden nodes on the 1st Ring. The results are shown in Figure 11.

Having three nodes on the 1st Ring that can not hear each other, as on Scenario A3, causes a great amount of collisions between them causing inefficiency on the network bottleneck which is the gateway neighborhood. On the contrary, when there are three nodes on the 1st Ring that can hear each other, the medium around the gateway is used more efficiently, leading to better network throughputs as shown by Figure 11.

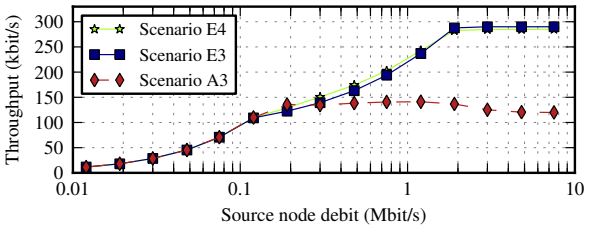

Fig. 11. Comparison of the throughputs of networks of Scenarios E4, E3 of Figure 9 and Scenario A3 of Figure 10.

V. Conclusions

Topology metrics related with hop count, neighbor node density, and hidden nodes were identified and studied with emphasis on how such metrics have been treated in previous works on wireless networks. These topology characteristics and metrics are treated separately in the literature. In this work, we address them jointly.

Extensive simulations using ns-2 were performed to evaluate the impact of topology characteristics on the throughput of a wireless mesh networks using two channels. The analysis of channel assignment schemes to a 36 node lattice gave important hints about the relative importance of network topology characteristics in network performance, namely:

1) the number of nodes around the gateway and the number of hidden nodes on the gateway neighborhood have a huge impact on the network performance, since the gateway neighborhood is the network bottleneck and it is important to use it efficiently;
2) the effects of hidden nodes measured by $miss\,ratio$ can be a significant metric when predicting the performance of a given topology;
3) mean hop count and neighbor node density has low impact on the network performance.

The experiments presented in this paper are enough to take conclusions about the impact of the topology characteristics described in Section II but, as future work, an extended set of random channel assignment schemes should be analyzed to get more generic conclusions. Since fairness is an important metric when characterizing the performance of a mesh network, it should also be addressed in future work. The joint study of fairness and throughput demands the definition of an utility function, so that the impact of topology characteristics on the network performance can be finally characterized. We belive that the knowledge obtained with this study can be applied to the efficient planning of single radio mesh networks.

References

[1] A. Abdullah, F. Gebali, and L. Cai. Modeling the throughput and delay in wireless multihop ad hoc networks. In *Proc. IEEE Global Telecom. Conf. (GLOBECOM'09)*, pages 1–6, USA, 2009.

[2] S. Avallone and I. F. Akyildiz. A channel assignment algorithm for multi-radio wireless mesh networks. *Computer Communications*, 31(7):1343–1353, 2008.

[3] J. Crichigno, M. Wu, and W. Shu. Protocols and architectures for channel assignment in wireless mesh networks. *Ad Hoc Networks*, 6(7):1051–1077, 2008.

[4] A. Dhananjay, H. Zhang, J. Li, and L. Subramanian. Practical, distributed channel assignment and routing in dual-radio mesh networks. *ACM SIGCOMM Computer Communication Review*, 39(4):99–110, 2009.

[5] P. Gupta and P. R. Kumar. The capacity of wireless networks. *IEEE Transactions on information theory*, 46(2):388–404, 2000.

[6] IEEE 802.11s. IEEE wireless LAN medium access control (MAC) and physical layer (PHY) specifications draft on mesh networking. 2009.

[7] L. B. Jiang and S. C. Liew. Improving throughput and fairness by reducing exposed and hidden nodes in 802.11 networks. *IEEE Trans. Mobile Computing*, 7(1):34–49, 2008.

[8] J. Jun, P. Peddabachagari, and M. Sichitiu. Theoretical maximum throughput of IEEE 802.11 and its applications. In *Proc. Inter. Symp. Network Computing and Applications (NCA'03)*, pages 249–256, USA, 2003.

[9] J. Jun and M. Sichitiu. The nominal capacity of wireless mesh networks. *IEEE Wireless Communications*, 10(5):8–14, 2003.

[10] M. Kodialam and T. Nandagopal. Characterizing the capacity region in multi-radio multi-channel wireless mesh networks. In *Proc. Inter. Conf. on Mobile computing and networking (MobiCom'05)*, pages 73–87, Germany, 2005.

[11] J. Kuo, W. Liao, and T. Hou. Impact of node density on throughput and delay scaling in multi-hop wireless networks. *IEEE Trans. Wireless Communications*, 8(10):5103–5111, 2009.

[12] P. Kyasanur and N. H. Vaidya. Capacity of multi-channel wireless networks: impact of number of channels and interfaces. In *Proc. Inter. Conf. on Mobile computing and networking (MobiCom'05)*, pages 43–57, Germany, 2005.

[13] J. So and N. Vaidya. Load-balancing routing in multichannel hybrid wireless networks with single network interface. *IEEE Trans. Vehicular Technology*, 55(3):806–812, 2006.

[14] R. Vedantham, S. Kakumanu, S. Lakshmanan, and R. Sivakumar. Component based channel assignment in single radio, multi-channel ad hoc networks. In *Proc. Inter. Conf. on Mobile computing and networking (MobiCom'06)*, pages 378–389, USA, 2006.

[15] K. Xu, M. Gerla, and S. Bae. How effective is the IEEE 802.11 RTS/CTS handshake in ad hoc networks. In *Proc. IEEE Global Telecom. Conf. (GLOBECOM'02)*, volume 1, pages 72–76, Taiwan, 2002.

Tânia Calçada received a Licenciatura (1999) degree in Electrical and Computer Engineering from Porto University. Previously she was working for a telecom operator designing corporate network solutions. Currently, she is a researcher at INESC Porto involved in projects related with mesh and vehicular networks. She is also currently involved in a PhD program on multi-channel assignment strategies for mesh networks.

Manuel Ricardo received a Licenciatura (1988), M.Sc. (1992), and Ph.D. (2000) degrees in Electrical and Computer Engineering from Porto University. Currently, he is an associate professor at the Faculty of Engineering, Porto University, where he gives courses in mobile communications and computer networks. He also leads Wireless and Mobile Networks area of INESC Porto (http://win.inescporto.pt/).